Meas. Sci. Technol. 5 (1994) 976–984. Printed in the UK

Design of a scanning probe microscope

H Olin

Department of Physics, Chalmers University of Technology, S-412 96 Göteborg, Sweden

Received 17 February 1994, in final form 14 April 1994, accepted for publication 18 April 1994

Abstract. A compact scanning probe microscope for operation in air and liquid is described. The probe techniques implemented are scanning tunnelling microscopy and scanning ion conductance microscopy. The software, electronics, mechanical construction and some representative measurements will be presented here. The compact and concentric microscope head is built around a commercial piezoelectric inchworm motor. The scanner is a standard piezo tube. An analogue feedback system is used for taking images, while digital control of the probe–sample distance is used for other experiments, such as measurements of current–voltage characteristics. A Macintosh personal computer is used for control and presentation of data. A simple method to make scanning tunnelling microscope tips suitable for electrochemical use is described. The microscope has a high resonance frequency (9.6 kHz), low noise (0.01 nm $Hz^{-1/2}$ at 10 Hz), low thermal drift (less than 0.1 nm min^{-1}), and high acoustical noise suppression. The current–distance-dependency of the scanning ion conductance microscope was found to be linear.

1. Introduction

Scanning tunnelling microscopes (STM) [1–4] and other scanning probe microscopes (SPM) [4, 5] give topographic images by scanning a tip over a sample, with resolution down to atomic dimensions. In the STM a conductive tip is brought close to (about 0.5 nm) the sample. When a small voltage is applied between the tip and the sample, a tunnelling current starts to flow. This current is strongly dependent on the distance and, by measuring the current, the tip–sample distance can be determined. The tip is then raster-scanned over the sample, while a feedback system keeps the tip–sample distance constant. A picture is generated by plotting this feedback signal.

The introduction of the STM in 1982 by Binnig, Rohrer and co-workers [6] has stimulated the development of other scanning probe microscopes, in which the tunnelling tip has been replaced by other probes, while keeping the rest of the concept. For example, in the scanning force microscope, electrostatic, magnetic or van der Waals forces are measured locally. Other SPMs measure local temperature, Faradaic currents or optical near fields. A great deal of work is being done to improve understanding of these probes and to implement new ones.

Another SPM, invented by Hansma and co-workers in 1989 [7], is the scanning ion conductance microscope (SICM). The probe in the SICM is an electrolyte-filled micropipette. The sample is immersed in an electrolyte and a voltage drives an ion current through the aperture of the pipette. The current decreases near the surface and the distance is monitored by measuring the current.

An SPM consists of four main parts: the probe, the mechanical parts, the electronics and the computer. The mechanical part consists of essentially a piezoelectric scanner, with a typical scanning range of a few micrometres, and a coarse positioning device that reduces the tip–sample to make it remain within the controlling range of the piezo. While the single piezo tube scanner invented by Binnig and Smith [8] has become a standard choice, a number of coarse positioning mechanisms have been implemented, for example, the early piezo electric walker ('the louse') [6], home-built [9] or commercial inchworms [10, 11], inertial gliders [12], lever reduced screw mechanisms [13] or differential screws [14]. For more examples and references, see [2, 15].

Because of the mechanical nature of these microscopes, one of the major construction problems is vibration isolation. The main noise sources are low-frequency building vibrations and sound. The general method [15, 16] to solve this problem is to construct the SPM with a high resonance frequency and to place it on a low-resonance-frequency damping table. An SPM with a high resonance frequency generally means a stiff and small SPM; the smaller the better. While the piezo scanner is small, the coarse approach mechanism usually adds to the size, and it is often the design of this mechanism that determines the overall vibration sensitivity. Thermal drift is another problem that must be considered in designing an SPM. This problem can be

0957-0233/94/080976+09$19.50

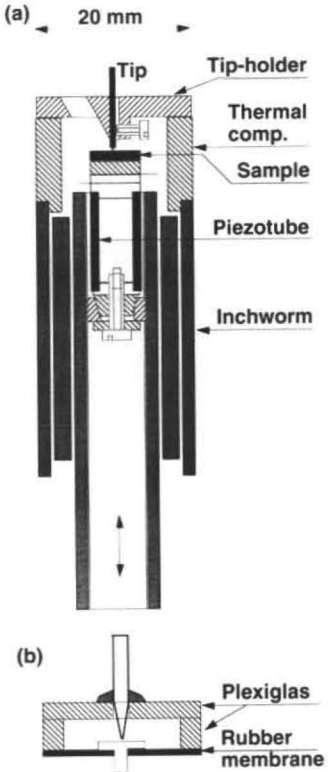

Figure 1. (*a*) The compact and axial symmetric microscope head is built around an inchworm motor. (*b*) When the microscope is operated in an electrolyte a small liquid cell is used. The liquid cell replaces the tip holder in (*a*).

solved by a symmetrical construction and careful choice of materials.

In this paper, we describe a scanning probe microscope for operation in air and liquid. The mechanical construction, electronics, software, probes and some representative measurements will be presented. The probes are STM tips and micropipettes for SICM use.

2. Mechanical

2.1. The mechanical loop

The compact microscope head (figure 1(*a*)) is built around a commercial piezoelectric inchworm motor (Burleigh Instruments, Inc), which is the coarse approach mechanism. The inchworm motor works by clamping and expansion/contraction sequence (figure 2). Each expansion is made in 2048 steps, giving a step size of 1 nm. The piezo scanner, with the sample holder, is fixed to the moving part of the motor. The tip holder is fixed to a thermal drift compensation tube, which is glued by epoxy resin directly onto the motor. This arrangement makes the mechanical loop very small.

2.2. Thermal drift

Lateral thermal drift is minimized by the axially symmetrical design of the SPM head. In the axial direction there is no such symmetry, and another

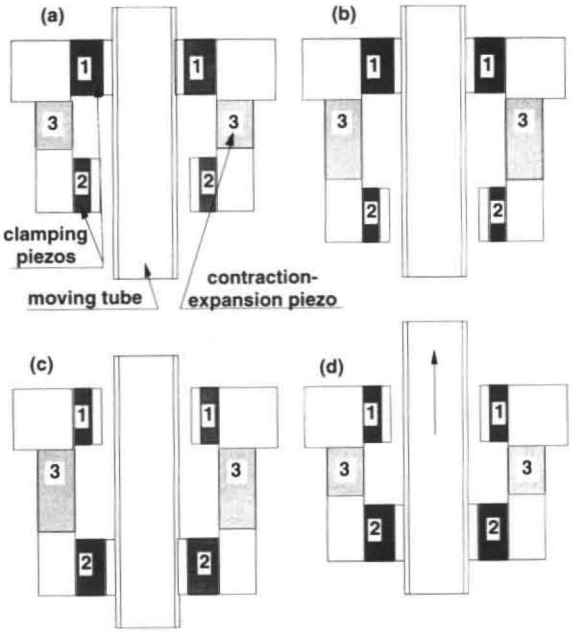

Figure 2. Principle of operation of the inchworm motor. (*a*) The inchworm is standing in the stop position. (*b*) Piezo 3 is expanding. (*c*) The lower piezo is clamped and the upper is released. (*d*) Piezo 3 is contracted, and the tube is moving up. The sequence is repeated from (*a*). Each cycle moves the tube about 2 μm.

approach is necessary. The piezo tube has a lower thermal expansion coefficient than the material used in the inchworm motor (aluminium oxide). To compensate for this a tube made of Invar is placed between the inchworm and the tip holder. The length of this thermal drift compensation tube has been calculated to match with a 2 mm tungsten tip and a 0.5 mm metal sample. The tip holder is fixed on the compensation tube by three screws. For observation of the tip and sample, the tip holder has an inspection hole (figure 1(*a*)).

2.3. Piezo scanner

The scanner is a standard single piezoelectric tube (PZT-5H [17]), which has an outside diameter of 6.35 mm, a length of 12.7 mm and a wall thickness of 0.56 mm. The tube has four outer electrodes and one inner electrode. Electrical wires are soldered on the electrodes at 150 °C using an indium solder. To improve the transient response behaviour, the tube was filled with silicon rubber as suggested by DiLella *et al* [18]. The tube is glued by epoxy resin onto an insulating glass ceramic disc (Macor, Corning). This disc is fixed on an expanding stainless steel mechanism, which is used to fix the scanner inside the moving part of the inchworm (figure 1(*a*)).

2.4. The sample holder

The sample holder is simply a screw, where the sample is fixed with conducting glue or with two small lever springs. To prevent leakage current and capacitive coupling from the piezo tube to the sample, a small stack

is glued onto the scanner. The stack consists of Macor, metal foil, Macor and stainless steel. The metal foil is earthed. The steel part has a thread, where the sample holder is screwed, and it is connected either to the bias voltage or to the current amplifier.

2.5. The liquid cell

To operate the microscope in a liquid, a small closed cell is used. The cell consists of a Plexiglas tip holder and a Plexiglas tube (3 mm high), onto which a flexible rubber membrane is glued (figure 1(*b*)). The membrane has a hole in the centre where the sample holder is placed and the connection is sealed with a nut on the back side of the membrane. The cell with the sample holder is screwed into the tube scanner and the cell is filled with liquid. The probe holder is placed on the top, and three screws seal the package. To prevent leakage of liquid, grease is placed between the probe holder and the Plexiglas tube. Two small holes are drilled in the tip holder to compensate for pressure changes. These holes are usually covered with grease to decrease evaporation of the liquid. The probe is glued onto the tip holder.

When the cell contains an electrolyte, it must be electrically shielded. It was found that the easiest and most effective way to eliminate electrical disturbances was to wrap the entire cell with a grounded or biased aluminium foil.

2.6. Vibration and sound isolation

For isolation of vibration and sound noise, the probe head is placed on a vibration damping stack, which hangs in thin rubber bands inside a closed box (figure 3). The damping stack consists of four stainless steel rings separated from each other by cut rubber tubes. This stack acts as a multistage mechanical low-pass filter [16, 19, 20].

On top of the stack a printed circuit board with electrical connectors is fixed. The electrical wires to the connectors are clamped to each ring to absorb vibrations. The SPM head has a similar board with connectors, making it possible to disconnect the head for replacement of sample and probe.

To suppress accoustical noise, it is important to use a closed box with thick walls made of a sound-absorbing material [21]. Stainless steel is a good sound-absorber, about half as good as lead, which is one of the best. Steel is easier to machine than lead and is also non-toxic, making it a good compromise.

In our case we used a closed cylindrical stainless steel box. The steel box has a 5 mm thick walls and to damp out resonances a 3 mm layer of rubber is added to the inside of all walls. The damping box can be used as it is or, better, placed on an additional damping system, which consists of a marble plate suspended from the ceiling by bunge cords.

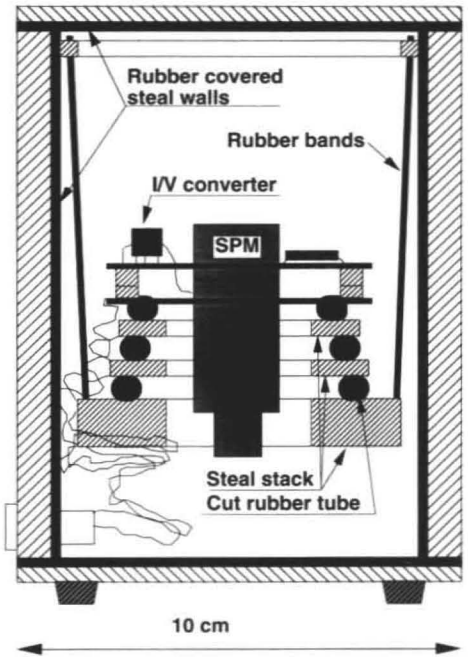

Figure 3. The vibration and sound damping box.

3. Electronics

The electronics consists of the current amplifier, the feedback system the piezo drivers and the inchworm electronics. An interface card is used for the connection between the electronics and the computer.

3.1. The current amplifier

The current amplifier (figure 4) is a high-impendance operational amplifier (OPA 128, Burr-Brown), where the current is converted to a voltage over a high resistance (1–1000 MΩ). The additional 10 kΩ resistor is for protection of the op-amp against accidental high currents. To minimize shunting capacitance contribution from the cable, the amplifier is placed on a circular printed circuit board directly on the SPM head, giving a cable length of 5 cm.

3.2. The feedback system

The amplifier probe signal is fed to the feedback system inside the main electronics box (figure 4). This signal is amplified 1, 10 or 100 times by an instrument amplifier (AD524). A logarithmic amplifier, AD755N, linearizes the exponential behaviour of the tunnelling current. The log-amp has an internal current source, which is used for the set point. This set point can be adjusted by the variable input resistor. The log-amp requires a negative input so a rectifier is necessary for operation with both negative and positive bias voltages. A modulator (AD630) is used as the rectifier [22]. The output from the log-amp is then fed to the integrator. The time constant may be adjusted by the variable resistor. Bias voltage is supplied by a 16-bit D/A converted from the card inside the computer. The bias is fed

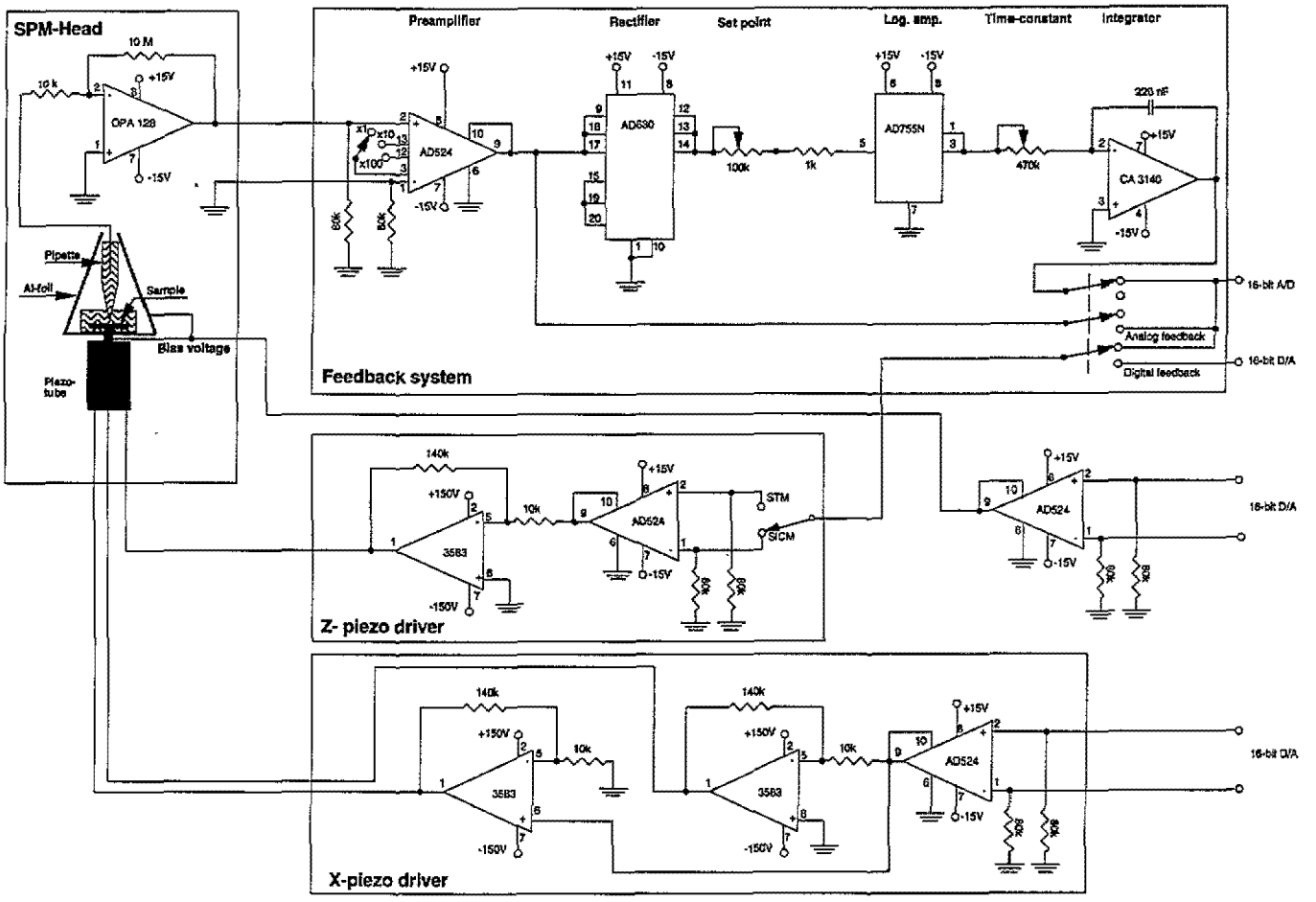

Figure 4. Circuit diagram of the feedback system and the current amplifier. The *y* piezo drivers (not shown) are identical to the *x* drivers.

through an instrument amplifier (AD524) to prevent ground loops and for suppression of common mode noise (this technique was used for all signals between different parts of the electronics).

When operating in the SICM mode the feedback output has to be reversed, because the signal is decreasing with decreasing tip–sample distance, not increasing as in the STM mode. This is done by a simple switch.

Another switch is used to connect a 16-bit D/A converter to the *z* piezo driver for computer control of the tip–sample distance. This allows computer-controlled feedback, and permits measurements of current–voltage and current–distance dependencies. It also permits alteration of the surface mechanically by gently pushing the tip into the surface.

3.3. Piezo drivers

The piezo scanner drivers are built around high-voltage operational amplifiers (CA3583, Butt-Brown), resulting in a simple design (figure 4). To prevent cross talk between the vertical and the lateral directions, we used symmetrical driving of the piezo tube by applying opposite voltages to oppose outer electrodes [23]. This also doubles the lateral scan range.

3.4. Inchworm electronics

The electronics for the inchworm motor is commercially available (6000 controller, Burleigh Instruments, Inc). The controller supplies the motor with high voltage (up to 700 V) signals. The controller was connected to three digital outputs from the interface card inside the computer to allow change in direction, clamping–unclamping in a stop position, and for stepping control.

The coarse approach was done by going towards the surface using the analogue feedback with the fastest response time. After contact, the motor continued to move until the *z* value was zero. The approach is controlled by the computer. For every 1 nm step, the feedback signal is checked, until the desired value is reached.

4. Computer and software

4.1. Computer and interface card

A personal computer (Apple Macintosh IIx, Motorola 68030 processor, 640 × 420 pixels, 8 bits, colour screen) was used for control of the probe measurement and for processing and presentation of data. A combination analogue and digital interface card (MacAdios II, with

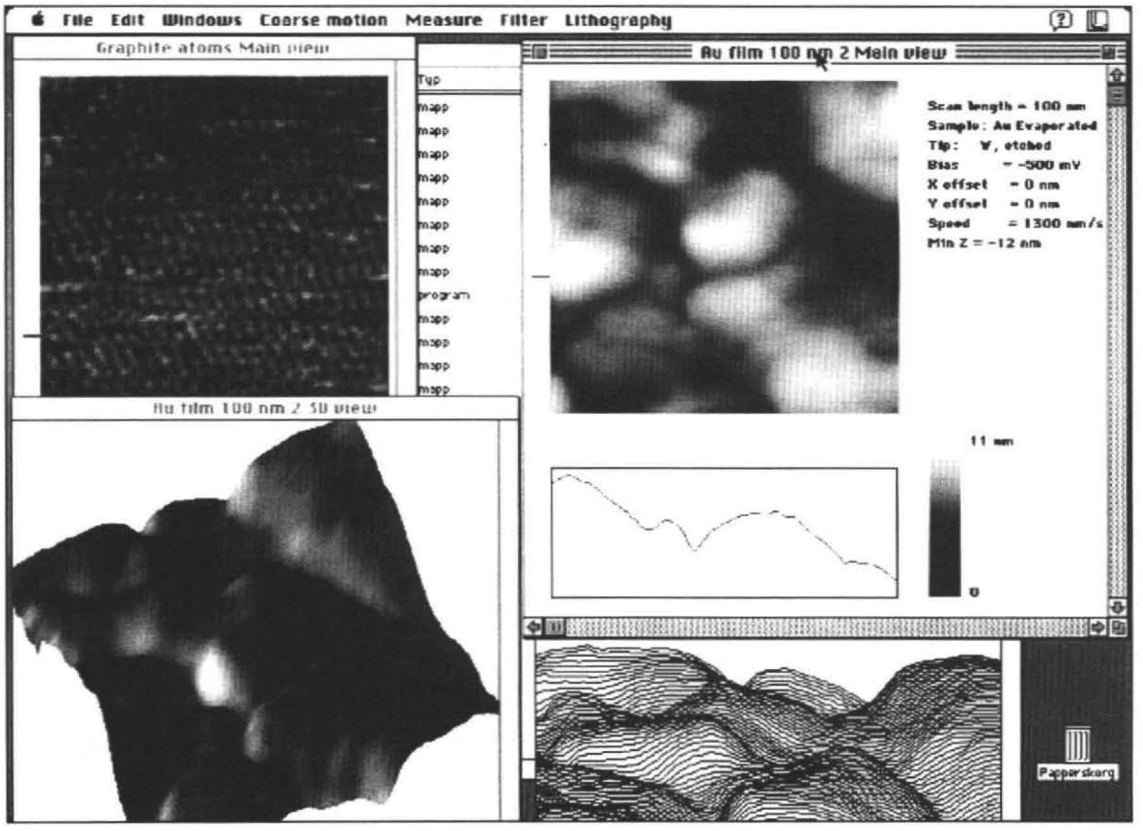

Figure 5. The user interface is built up with curtain menus, multiple windows and dialogues. This screen dump shows four windows. One is showing a grey scale image of graphite with atomic resolution taken in the constant current mode. The other three windows show an evaporated film of Au–Pd in three different views. The views are grey scale, solid three-dimensional and line plot views.

one 16-bit analogue input and two 16-bit analogue output baby boards. GW Instruments, Inc) was used for the interface to the analogue electronics and to the inchworm electronics. The feedback signal is connected to the 16-bit A/D input, which gives a resolution of 0.2 Å bit^{-1} in the z direction. The 16 bit D/A output gives a resolution of 0.4 Å bit^{-1} in the lateral directions. The conversion rate is 50 kHz.

4.2. The development system

The software was written in Object Pascal using MacApp and the software development tools in the Macintosh Programmers Workshop (Apple Computer Inc). MacApp is an almost complete, generic Macintosh program ready to customize. MacApp could also be considered as a set of reusable libraries upon which to base the new program. MacApp is written in Object Pascal. An object is like a small program, which contains both the data and the routines that operate on the data. To customize MacApp and build a new program, some objects are changed and new ones are created. The advantage with object oriented programming, as compared with procedure oriented, is that it is easy to reuse old codes.

4.3. Picture measuring routines

To scan the piezo in the x direction, a voltage ramp from the D/A converter is needed. The values of the ramp are stored in a memory array, and to make the ramp as smooth as possible, all bits are used, resulting in step sizes of 0.4 Å. An input array, with the same size as the output array, is allocated to hold the measured data. The output and the simultaneous input are controlled by a clock on the interface card. This also allows the scan speed to be controlled, a parameter better suited than the scan frequency, which is commonly used. The measured information is placed in an allocated picture memory after each scan. The y movement is made by a simple loop, with single bit steps. The same technique is used to offset the tip to another start position.

4.4. Digital feedback

Digital feedback allows more flexible use of the microscope than does analogue feedback, but it is also more difficult to achieve because of the amount of computation involved. A simple routine is implemented for digital feedback. Depending on the value of the tunnelling current, the distance is unchanged or changed by a single bit (corresponding to 0.2 Å). Two current values are defined, a top value and a bottom value.

When the current exceeds the top value, the tip–sample distance is increased, and when the current is below the bottom value, the distance is decreased. The top value is not equal to the bottom value, so there is a window between the two in which the distance is not changed. The reason for this perhaps odd algorithm is that it was found to be more stable than an ordinary PI-regulator. A similar approach, which was implemented in hardware, has given a much higher speed [24].

Our implementation was found to be too slow for image measuring, but for other purposes, such as measuring I–V and I–z curves, it was found to be convenient. This was also necessary because there is no sample-and-hold circuit in the electronics. Differentiation of I–V curves was performed by a simplified least squares procedure [25].

4.5. The user interface and picture presentation

The user interface was implemented in the standard Macintosh way with curtain menus, windows (figure 5) and dialogues. Several routines are implemented for presentation of the pictures. The most useful is the top view in which the height information is put into a grey scale. The grey scale image is complemented with a moving marker, which points to a single image line. This line is plotted below the image, giving a cross sectional view of this particular line.

For three-dimensional image presentation, a hidden line algorithm and a colour solid surface algorithm are used. The latter is made by simply drawing the lines of the picture with a wide vertical coloured pen, and by drawing from top to bottom there is no need to hide the previous lines. The colour of the pen is picked from the slope of the lines, giving the picture a simple shading. The slope is calculated by the same least squares algorithm as mentioned above [25]. The colours can be selected from a number of predefined colour tables of customized by picking colours from a palette.

4.6. Filtering

A number of filtering and image modification routines are implemented. The most important one is the plane-adjust algorithm. Another routine, that is useful when there are spikes in the picture, is a line-removal algorithm. The user picks a bad line and this is replaced by the average of the two nearest lines. A simple low-pass filter is implemented, this is done by replacing each picture point value by the average of the point value and the values of the nearest neighbours.

4.7. Hard copies

Hard copies of the images were obtained with a standard laser printer. Although the program contains printer routines, it was found convenient to make screen dumps, and use the standard Macintosh cut and paste commands to place images into image processing programs (namely Adobe Photoshop) or word processors for documentation.

5. Probes

The probes used in this microscope were STM tips for use in air and in electrolyte, and micropipettes for SICM use. The tunnelling tips in air were all standard [26, 27] etched tungsten or etched or cut Pt–Ir tips.

5.1. The STM tips

The tunnelling tips used in water and electrolyte had to be partly covered by an insulator to prevent high Faradaic currents. For distilled water commercially available glass and epoxy covered tips (Longreach Scientific Resources Inc) were found to be suitable. The exposed area, however, gave Faradaic currents that were too large for proper operation in an electrolyte. Therefore a new method was used that gives a very small exposed area. The method is simple: first cover the entire tip with a low viscous cyanoacrylate glue and then use the STM to press the tip against a gold film until a tunnelling current is detected. These tips give a very small Faradaic current (less than 0.1 nA at 100 mV bias voltage in 1 M KCl) and are suitable for operation in an electrolyte. These tips were used successfully to image a gold film and a silver surface. A similar, but more complicated, method has been described by Heben *et al* [28]. They covered the tips by glass or polymer in a specially designed apparatus.

5.2. Micropipettes

For operation in the SICM mode we used standard micropipettes, which are used in measurements of intracellular potentials and in the patch-clamping technique. The pipettes were fabricated in a commercial pipette puller. Capillary glass tubes (2 mm outer diameter, 1 mm inner) are clamped at both ends and electrically heated in the middle, the tube is then pulled aside giving two micropipettes. The aperture diameter of a pipette was estimated by using a light microscope. A typical aperture diameter was 1 μm and outer diameter 2 μm. The pipettes were filled with 1 M KCl by capillary action. The liquid cell was also filled with 1 M KCl to avoid concentration potentials. Reversible Ag/AgCl electrodes were used as electrodes both in the pipettes and in the bath. Typical voltages and currents were 100 mV and 100 nA.

6. Performance and discussion

We have used this microscope in the STM mode in a number of measurements, for example, on high-temperature superconductor (YBCO) thin films [29] and on oxidized titanium [30]. Characteristic features of the microscope and measurements in the SICM mode are reported here.

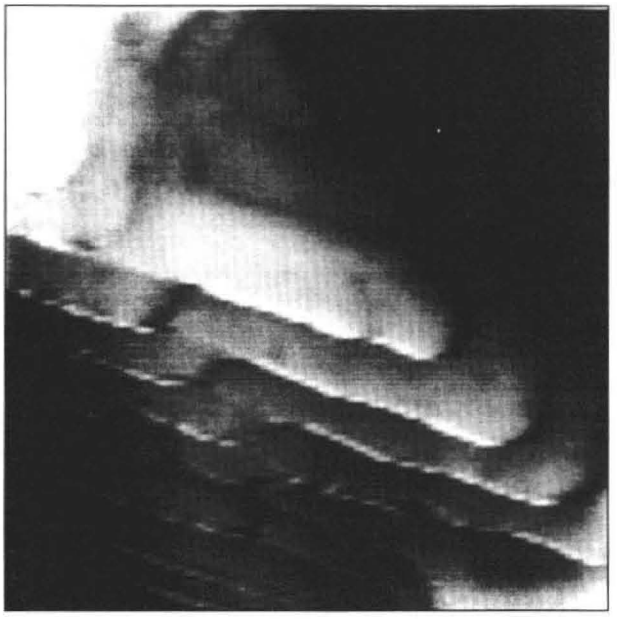

Figure 6. A scanning tunnelling microscopy grey-scale picture of a laser-deposited high-temperature superconductor $YBa_2Cu_3O_{7-x}$ thin film. The layered structure is visible, with unit cell steps (1.2 nm). The image size 100 nm×100 nm.

6.1. Piezo calibration

We calibrated the piezo scanner in the lateral directions by imaging graphite atoms and in the z direction by imaging the layered structures of laser-deposited high-temperature superconducting YBCO thin films (figure 6). The motion versus voltage in the vertical direction was 5 nm V^{-1} and in the lateral directions 10 nm V^{-1}. An additional lateral calibration was done using a gold grating, with a 200 nm lattice spacing, giving results consistent with the graphite measurements. With micrometre-sized offsets and scans, however, a considerable amount of creep was present. Creep, an intrinsic property of these piezo ceramics, is a slow additional response after a voltage step and it continues in a logarithmic way [31].

6.2. The inchworm motor

When the desired tip position is found using the inchworm motor, the upper clamp is supposed to be closed as in figure 2(*a*). However, when this stop-clamping was executed, contact between tip and sample was lost in almost all cases. This means a movement of almost 1 μm in the z direction. The reason for this malfunction is probably that the tip is moved laterally. This motion is much faster than the response of the feedback system and a tip crash is very probable. Therefore, the stop possibility was seldom used. Instead the motor was standing in the ready postion and, because of this, the noise in the expansion piezo of the motor (3 in figure 2) was added to the other noise sources in the microscope. To overcome this problem, a less noisy motor driving electronics and a smoother clamping could be used [11].

Another way around the problem with the noise motor is to use a different design of the head. The motor could be used just to push and pull on a sliding part that holds the piezo scanner. When the probe is properly positioned, the motor could be slightly retracted and the contact between the motor and the sliding part is broken. Similar designs have been described by, for example, Bando *et al* [14], who used a differential screw as the pusher.

6.3. Instrument noise

The resonance frequency was measured by exciting the piezo in the positive x direction with a 10 V sine wave signal and measuring the voltage on the negative x electrode. The frequency was increased until the piezo started to resonante. This gave a resonance frequency of 9.6 kHz. The mechanical noise level was measured by making a spectrum analysis of the z voltage using a cut Pt–Ir tip and a gold film as the sample and with the damping box standing on an ordinary table. The tip bias was 100 mV and the tunnelling current 1 nA. The spectrum analysis program was written in LabView (National Instruments Inc). The noise was found to have a $1/f$ noise and a white noise contribution of about 0.01 nm $Hz^{-1/2}$. This noise level was lowered by about 50% when the motor controller was turned off.

6.4. Acoustical noise

Acoustical noise suppression was very high. The standard trick of clapping hands had no effect on the tunnelling current, not even musical equipment playing at high volume showed any detectable effect.

We have obtained similar results with the same technique using a commercial microscope (Nanoscope III, Digital Instruments), which was sensitive to sound noise. This box was larger (about 0.2 m^3) and a less good sound absorbing material (aluminium) was used. However, the same technique of disconnecting the microscope head from the walls, by hanging it in rubber bands inside the box, was used.

6.5. Thermal drift

Thermal drift in the z direction was measured by turning off the driving electronics of the inchworm motor and then waiting for 1 h for the piezoelectric creep in the inchworm and the piezo scanner to relax. The drift was less than 0.1 nm min^{-1}. In one experiment, a gold film was investigated for 2 weeks without moving the motor at all. The lateral thermal drift was estimated by taking 50 nm sized images of the gold film at 10 min intervals. The drift was less than 0.1 nm min^{-1}.

6.6. The SICM

The dependence of conductance on distance in the SICM had not been measured earlier. To measure this, the feedback loop was opened, and the ion current was

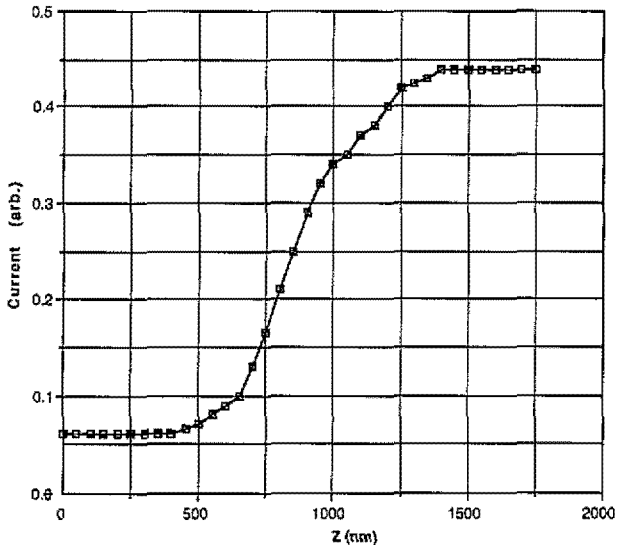

Figure 7. Measurement of the ion current versus distance in the scanning ion conductance microscope, showing the linear dependency. The high constant value is the bath value and the low constant value is a background current when the tip is pressed into the sample (a leaf).

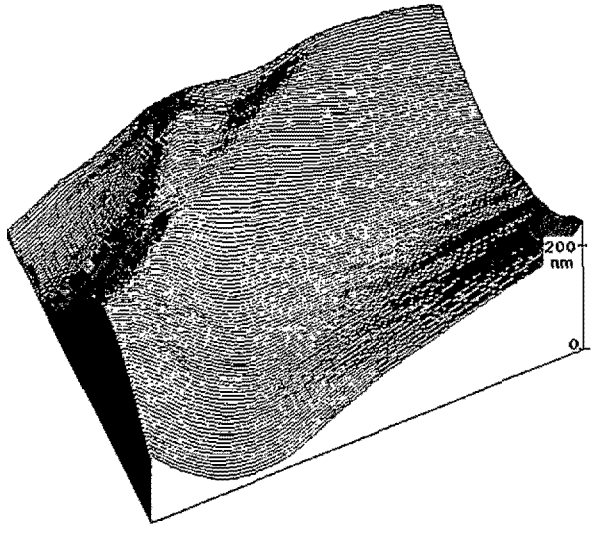

Figure 8. A scanning ion conductance microscopy line plot picture of a leaf. The aperture diameter of the pipette used was 1 μm, The scan size is 2.8 μm×2.8 μm.

measured at 100 nm intervals by moving the sample (a leaf in this case) with the motor towards the tip. The aperture of the pipette had an inner diameter of 1 μm. The current was found to be linearly dependent on the distance (figure 7). From the curve it is evident that the most distance-sensitive position of the current is where the current is about half the bath value (the value of current when the tip is far from the surface).

Figure 8 shows a SICM image, taken with a pipette with an opening diameter of 1 μm and with the current set to half the bath value. The resolution of the SICM has been estimated to be of the same order as the aperture diameter [7].

To increase the resolution in the SICM the diameter of the aperture of the micropipette should be reduced. However, with decreased diameter the pipettes become fragile and break easily as observed by Hansma *et al* [7]. The same group made more stable tips by microfabrication techniques, giving openings down to 200 nm [32]. We are also working in this direction and have, using another microfabrication technique, made pipettes with an aperture down to 10 nm. Work is in progress to use them in this microscope.

7. Conclusion

A compact, cylindrically symmetric, scanning probe microscope, with a high resonance frequency (9.6 kHz), low noise level (0.01 nm $Hz^{-1/2}$ at 10 Hz), low thermal drift (less than 0.1 nm min^{-1}) and high sound noise suppression, has been constructed. A simple method to make electrochemical tips, giving a Faradaic current less than 0.1 nA, has been described.

Operation in the SICM mode was demonstrated, and the distance-dependency of conductance in the SICM was found to be linear.

Acknowledgments

I thank M Stenberg for close collaboration on the SICM work. The work was supported by the Swedish Board for Industrial and Technical Development and by the Technical Science Research Council.

References

[1] Binnig G and Rohrer H 1986 Scanning tunneling microscopy *IBM J. Res. Dev.* **30** 355

[2] van de Leemput L E C and van Kempen H 1992 Scanning tunnelling microscope *Rep. Prog. Phys.* **55** 1165

[3] Güntherodt H-J and Wiesendanger R (eds) 1992 *Scanning Tunneling Microscopy I. General Principles and Applications to Clean and Adsorbate-covered Surfaces* (Berlin: Springer)

[4] Güntherodt H-J and Wiesendanger R (eds) 1992 *Scanning Tunneling Microscopy II. Further Applications and Related Techniques.* (Berlin: Springer)

[5] Wickramasinghe H K 1990 Scanning probe microscopy – current status and future trends *J. Vac. Sci. Technol.* A **8** 363

[6] Binnig G, Rohrer H, Gerber C and Weibel E 1982 Surface studies by scanning tunneling microscopy *Phys. Rev. Lett.* **49** 57

[7] Hansma P K, Drake B, Marti O, Gould S A C and Prater C B 1989 The scanning ion-conductance microscope *Science* **243** 641

[8] Binnig G and Smith D P E 1986 Single-tube 3-dimensional scanner for scanning tunneling microscopy *Rev. Sci. Instrum.* **57** 1688

[9] Besenbacher F, Laegsgaard E, Mortensen K, Nielsen U and Stensgaard I 1988 Compact, high-stability, thimble-size scanning tunneling microscope *Rev. Sci. Instrum.* **59** 1035

[10] Rosolen G C and Welland M E 1992 A combined scanning electron microscope and scanning tunneling microscope for studying nanostructures *Rev. Sci. Instrum.* **63** 4041

[11] Jeon D and Willis R F 1991 Inchworm controller for fine approach in a scanning tunneling microscope *J. Vac. Sci. Technol.* A **9** 2418

[12] Pohl D W 1987 Dynamic piezoelectric translation devices *Rev. Sci. Instrum.* **58** 54

[13] Drake B, Sonnenfeld R, Schneir J and Hansma P K 1987 Scanning tunneling microscopy of processes at liquid solid interfaces *Surf. Sci.* **181** 92
[14] Bando H, Morita N, Tokumoto H, Mizutani W, Watanabe K, Homma A, Wakiyama S, Shigeno M, Endo K and Kajimura K 1988 Scanning tunneling spectroscopy study on graphite and 2H-$NbSe_2$ *J. Vac. Sci. Technol.* A **6** 344
[15] Kuk Y and Silverman P J 1980 Scanning tunneling microscope instrumentation *Rev. Sci. Instrum.* **60** 165
[16] Pohl D W 1986 Some design criteria in scanning tunneling microscopy *IBM J. Res. Dev.* **30** 417
[17] EBL Division, Staveley Sensors Inc, East Hartford, Connecticut 06108, USA
[18] DiLella D P, Wandass J H, Colton R J and Marrian C R K 1989 control-systems for scanning tunneling microscopes with tube scanners *Rev. Sci. Instrum.* **60** 997
[19] Oliva A I, Sosa V, de Coss R, Sosa R, Salazar N L and Pena J L 1992 Vibration isolation analysis for a scanning tunneling microscope *Rev. Sci. Instrum.* **63** 3326
[20] Schmid M and Varga P 1992 Analysis of vibration isolation system for scanning tunneling microscope *Ultramicroscopy* **42–44** 1610
[21] Thumann A and Miller R K 1990 *Fundamentals of Noise Control Engineering* 2nd edn. (Lidburn, CA: Fairmont)
[22] Park S I and Quate C F 1987 Scanning tunneling microscope *Rev. Sci. Instrum.* **58** 2010
[23] Besocke K 1987 An easily operable scanning tunneling microscope *Surf. Sci.* **181** 145
[24] Robinson R S , Kimsey T H and Kimsey R 1991 Desktop computer-based management of images and digital electronics for scanning tunneling microscopy *J. Vac. Sci. Technol.* B **9** 631
[25] Savitzky A and Golay M J E 1964 Smoothing and differentiation of data by simplified least squares procedures *Anal. Chem.* **36** 1627
[26] Garnaes J, Kragh F, Mørch K A and Thölén A R 1990 Transmission electron-microscopy of scanning tunneling tips *J. Vac. Sci. Technol.* A **8** 441
[27] Melmed A J 1991 The art and science and other aspects of making sharp tips *J. Vac. Sci. Technol.* B **9** 601
[28] Heben M J, Quate C F, Penner R M, Lewis N S and Dovek M M 1988 Preparation of STM tips for *insitu* characterization of electrode surfaces *J. Microsc.* **152** 651
[29] Olin H, Brorsson G, Davidsson P, Ivanov Z G, Nilsson P Å and Claeson T 1992 Scanning tunneling microscopy of laser deposited YBCO thin films *Ultramicroscopy* **42–44** 734
[30] Olin H, Aronsson B O, Kasemo B, Lausmaa J and Rodahl M 1992 Scanning tunneling microscopy of oxidized titanium surfaces in air *Ultramicroscopy* **42–44** 567
[31] van de Leemput L E C, Rongen P H H, Timmerman B H and van Kempen H 1991 Calibration and characterization of piezoelectric elements as used in scanning tunneling microscopy *Rev. Sci. Instrum.* **62** 989
[32] Prater C B, Hansma P K, Tortonese M and Quate C F 1991 Improved scannning ion-conductance microscope using microfabricated probes *Rev. Sci. Instrum.* **62** 2634